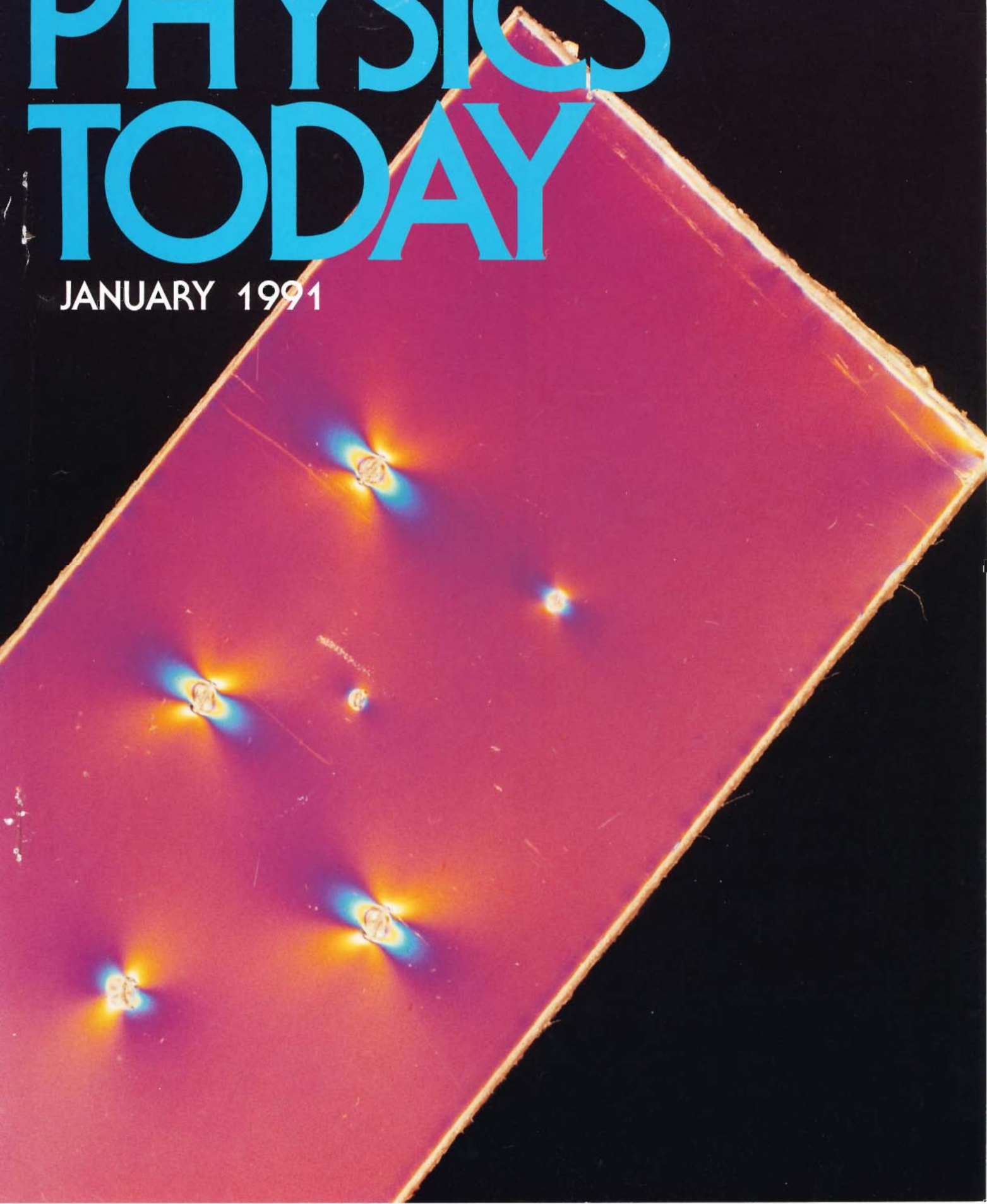


PHYSICS TODAY

JANUARY 1991



TIME-SCALE INVARIANCE IN TRANSPORT AND RELAXATION

Important, and often puzzling, features of transport and relaxation in disordered systems can be attributed to the long-tailed distributions of the times between events that limit the motion.

Harvey Scher, Michael F. Shlesinger and John T. Bendler

An early theme in probability was calculating the fair ante for various games of chance. Nicolas Bernoulli introduced a seemingly innocent game, first published in 1713, that yielded a paradoxical result. The result has become known as the St. Petersburg paradox, because of an analysis written later by Daniel Bernoulli in the *Commentary of the St. Petersburg Academy*.¹

Flip a coin. If it comes up heads, then you win one coin. If it comes up tails, flip again until a head appears. If N tails precede a head, then you win 2^N coins. Each such event occurs with probability $1/2^{N+1}$. The mean winnings are therefore $\frac{1}{2} \times 1 + \frac{1}{4} \times 2 + \frac{1}{8} \times 4 + \dots = \infty$. The house wants you to ante an infinity of coins (the house's expected loss). You counter that a smaller ante is in order because your median winnings are only one coin and to win an infinity of coins you must flip an infinity of times, which is unreasonable.

The paradox arises from trying to determine a characteristic size from a distribution that does not possess one. Winnings occur on all scales, with an order of magnitude greater winning occurring an order of magnitude less often. The lesson to be learned from the St. Petersburg paradox is that one should work *directly with the probability distribution*, and not just with its moments. This will be a dominant theme in this article.

If the first moment (the mean) of a probability distribution exists, it defines a scale. While one major thrust of physics is to find the right scale for a problem—the size of an atom, the mobility of an electron in a crystal—a newer thrust is to investigate problems that have no characteristic scale. In critical phenomena, the struggles and successes in tackling scale-invariant problems where correlation lengths diverge are well known.

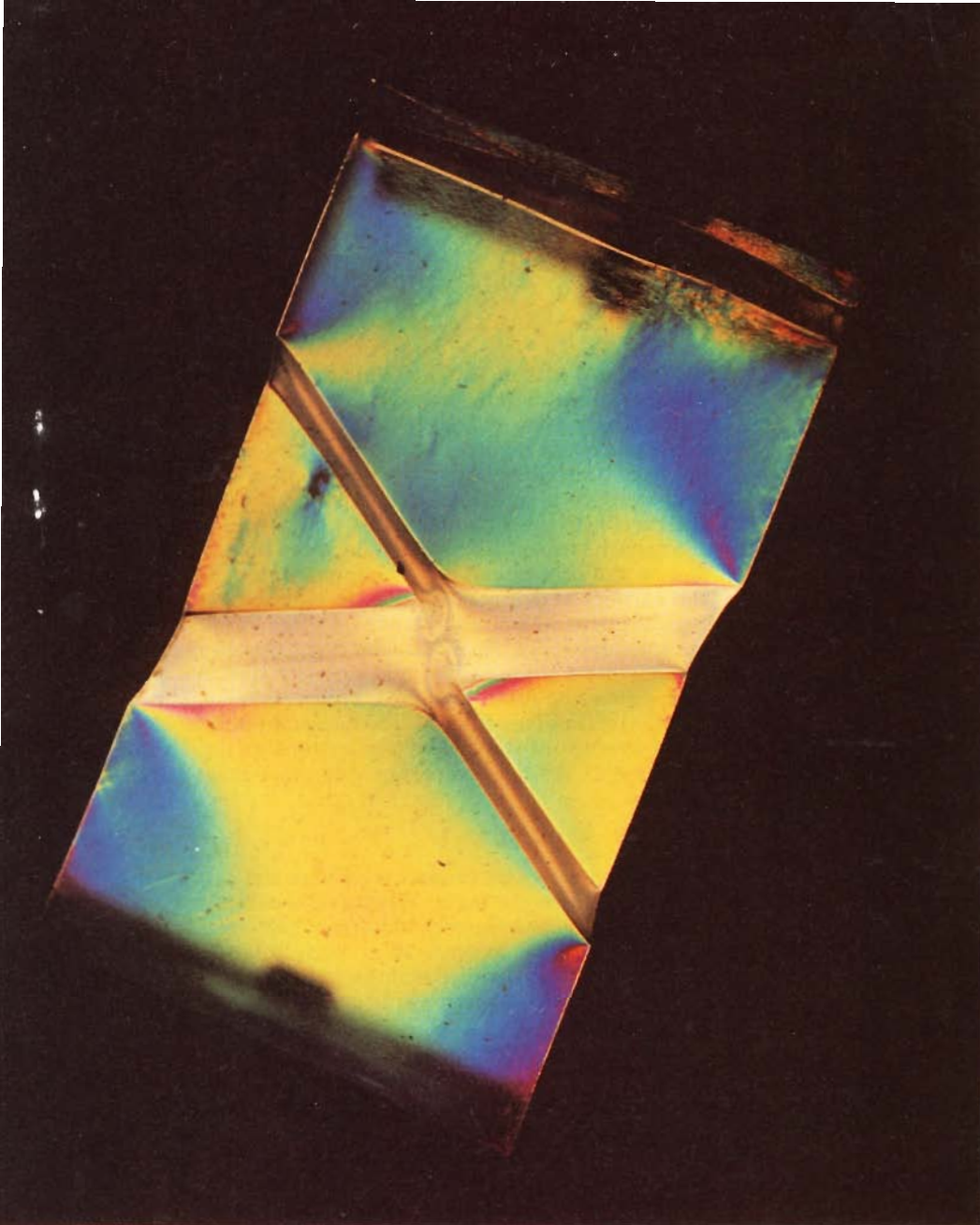
Harvey Scher is a senior research associate at BP Research, in Cleveland, Ohio. **Michael Shlesinger** is director of the physics division of the Office of Naval Research, in Arlington, Virginia. **John Bendler** is a staff physicist at the General Electric Company, in Schenectady, New York.

In this article we are interested in microscopic processes that do not possess a characteristic time scale. We will focus on transport and relaxation in disordered solids when the mean-waiting-time scale between events—electron hopping, defect movement and so on—diverges. Transport governed by such a long-tailed waiting-time distribution is called “dispersive” because many time scales coexist.

Scale-invariant dynamic phenomena are seen in a wide variety of disordered materials. Dispersive motion can account quantitatively for many of the universal characteristics seen in transport and relaxation measurements in these materials, which include amorphous semiconductors and insulators, polymer films (see figure 1), molecular solid solutions and glasses. We begin our treatment of these topics with a discussion of charge transport in disordered semiconductors and close with an extension of the above ideas to “stretched exponential” relaxation in glassy materials.

Dispersive transport

The movement of electrons in disordered systems is a paradigm of long-tailed distributions and is easily measured. A common example is transport via a sequence of charge-transfer steps from one localized site to another in the presence of an applied electric field. The process is called “trapping” if the transfer step involves thermal activation from the site to a conduction band, in which the charge diffuses to the next site. Tunneling directly between localized sites is known as hopping. Figure 2 shows these processes schematically. Due to the disorder, the transfer time can be a random variable, characterized by the probability $\psi(t) dt$ that the time for an individual transfer (or event) is between t and $t + dt$. The accumulated sequence of these events in the motion of a charge carrier can be viewed as a continuous-time random walk.² By specifying the probability distribution $\psi(t)$ and the spatial bias introduced by the electric field, one can calculate the properties of a packet of charge propagating across a sample.³



Strain birefringence in plastically deformed polycarbonate, viewed in plane-polarized light. The arms of the cross are composed of cold-drawn resin. The more intensely colored regions surrounding the cross are sheared polymer. Such optical techniques for measuring strain have been used in conjunction with mechanical studies to verify the Kohlrausch law for relaxation and recovery in a wide number of thermoplastics. (See the box on page 34.) **Figure 1**

Time-of-flight measurements. The canonical technique for measuring electron transport is the time-of-flight experiment. A pulse of strongly absorbed light, incident near an electrode, generates nonequilibrium electrons and holes. In the polarity shown in figure 3, the electrons are swept into the near electrode, leaving a sheet of holes to move to the far electrode; this motion gives rise to a current $I(t)$ in the external circuit. The current $I(t)$ in the sample has two contributions, the conduction current $j_c(x,t)$ and the displacement current. One integrates over the sample thickness d to obtain

$$I(t) = \frac{1}{d} \int_0^d j_c(x,t) dx + \frac{\epsilon}{d} \frac{dV}{dt} \quad (1)$$

Here V is the voltage across the sample and ϵ the dielectric constant. When a constant voltage V is maintained we see that $I(t)$ is the space average of the conduction current. Thus the holes do not have to be collected at the far electrode to generate a current in the circuit; changes in the field across the sample induced by the moving holes generate a current as the battery attempts to maintain a constant voltage.

Curve 1 in figure 3 shows the expected result for the current $I(t)$ due to normal transport. The velocity of the sheet of holes is constant; therefore the current is constant until the holes are absorbed at the electrode, at which time they no longer contribute to the current. The "transition region," over which the current drops to zero, is a measure of the spread in the hole packet due to normal diffusion.

Early experiments done in the late 1960s revealed rather bizarre current traces. Standing in sharp contrast to the current trace shown in curve 1 is curve 2, measured by Merle Scharfe of Xerox for amorphous As_2Se_3 , a material then used as a photoconductor in photocopy machines.⁴ Not only does the current $I(t)$ decrease over the entire time of flight (except for a small "plateau" region), but the particular shape of this decay is scale invariant. A scale is defined by the transit time t_r , corresponding to the onset of the long tail. For a given material, $I(t)/I(t_r)$ vs t/t_r is independent of t_r . In the same relative units, the shape of the "normal" current trace would depend explicitly on the transit time t_r , because the width of the region of constant current increases linearly with t_r , while the "transition region" increases only as $\sqrt{t_r}$.

Further, using the usual definition of the drift mobility,

$$\mu_d = d/(t_r E) \quad (2)$$

where E is the applied electric field, one observes μ_d to depend inversely on the sample thickness! These facts remained a puzzle until a fundamentally new theory clarified both the phenomenon and the expected form of the experimental trace.

Random-walk theory. This new theory assumed that each charge carrier independently undergoes a random walk biased in a preferred direction by the applied field. The entire character of the propagating packet of charge depends on one key feature of the probability distribution $\psi(t)$: If the first two moments of $\psi(t)$ exist, the transport is normal, as in curve 1 of figure 3. If the first moment $\langle t \rangle$ of $\psi(t)$ does not exist, the charge packet can still transit the sample; however, it exhibits an unusual dispersion. For a probability distribution $\psi(t)$ with an algebraic tail given by

$$\psi(t) \sim t^{-(1+\beta)} \quad (3)$$

one has $\langle t \rangle = \infty$ for $\beta \leq 1$ (β must be greater than 0 for $\psi(t)$ to be normalizable). The mean position of the spatially biased time-evolving packet then varies as

$$l(t) \propto l(E) t^\beta \quad (4)$$

This is discussed in the box on page 30, which outlines how to deal mathematically with an infinite first moment $\langle t \rangle$; $l(E)$ is the mean step displacement. This sublinear variation in time is the key to all the peculiar features of the current $I(t)$ discussed above. Once we have demonstrated this central point, we will discuss how the distribution in equation 3 arises naturally in disordered systems.

Figure 4 contrasts the packet propagations $P(l,t)$ for two types of probability distributions $\psi(t)$ that have the same spatial bias due to the electric field. The normal (Gaussian) transport and diffusion result from a $\psi(t)$ with finite first and second moments. The Gaussian behavior is a consequence of the well-known central limit theorem. The position of the peak of the distribution coincides with the spatial mean $l(t)$. This is not the case for the packet propagation $P(l,t)$ generated by the algebraic distribution

in equation 3 with $\beta \leq 1$. With increasing time, the peak of this $P(l,t)$ remains at the initial position, while the mean is continuously displaced from it. This unusual behavior originates in the relatively small, but finite, probability of an event time that is much larger than a typical one. Because such a rare, but quite long, event time can be comparable to the accumulation of typical event times in the carrier's transit across a sample, it can have a large effect on the carrier motion. The forward "streaming" of the carriers is due mainly to those carriers undergoing typical events. Eventually, many of these forward carriers will experience one of the long event times. Thus the mean position of the packet increases with time, but at an ever decreasing rate. The mean is therefore a sublinear function of time (equation 4). The measured current is the space average of the conduction current in the sample (equation 1), which is proportional to the average packet velocity:

$$I(t) \propto dl(t)/dt \sim t^{-(1+\beta)}, \quad t < t_r \quad (5)$$

Hence the current decreases even before the carriers are absorbed into the electrode. When a reasonable fraction of the carriers (approximately 10%) reach the electrode, the current begins to decrease at a faster rate due to the carrier loss. The detailed solution³ to the problem of a random walk with a bias toward an absorbing plane shows a crossover to

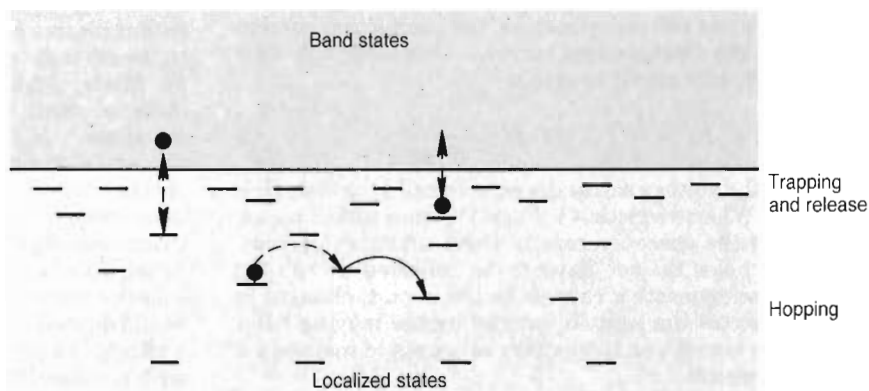
$$I(t) \sim t^{-(1+\beta)}, \quad t > t_r \quad (6)$$

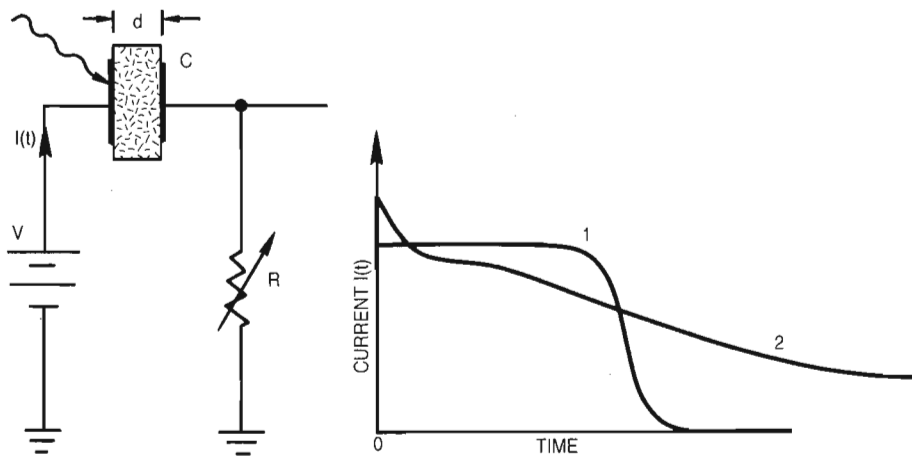
A double logarithmic plot of the current $I(t)$, corresponding to equations 5 and 6, is simply two lines with slopes $-(1-\beta)$ and $-(1+\beta)$, separated by a narrow transition region. Note that the sum of the slopes is -2 , independent of the exponent β that defines the algebraic probability distribution! An estimate for the transit time t_r , which denotes the transition region from slope $-(1-\beta)$ to $-(1+\beta)$, is easily obtained from the relation $l(t_r) \sim d$ or, using equation 4,

$$t_r \sim [d/l(E)]^{1/\beta} \quad (7)$$

(Typically, $l(E)$ is proportional to E .) Using equation 2 as a definition of mobility for this dispersive transport, one then has a field- and thickness-dependent drift mobility

Energy levels in an amorphous semiconductor. This schematic diagram illustrates band transport with trapping, and hopping transitions between localized states in the energy gap. **Figure 2**





Transient photocurrent or time-of-flight experiment scheme, and plot of results. A light flash of duration less than the transit time t_t is incident on a semitransparent electrode and is absorbed in a depth of the dielectric much smaller than the sample thickness d . Carriers of one sign move across the sample, inducing a time-dependent current $I(t)$ in the external circuit. Curve 1 is a typical current trace measured in a material with a well-defined mobility. The transit time t_t is the time for the current to drop to one-half of its upper-plateau value. Curve 2 is a highly dispersive transient photocurrent trace measured in As_2Se_3 by Merle Scharfe of Xerox.⁴ **Figure 3**

μ_d . This anomalous dependence illustrates that in a system with time-scale invariance there are no intrinsic transport coefficients. External parameters such as sample thickness constrain the dynamic response of the system, and hence these limit the “transport coefficients”—that is, they become laboratory-time dependent!

The theory embodied in equations 5–7 predicts both the shape of the transient current and the relation between this shape and the dependence of the transit time on the sample thickness and field—namely, that the values of the exponent β determined from the shape and from the transit-time dependence are the same. This relationship is a hallmark of dispersive transport.

Experiments and mechanisms

These relationships were dramatically confirmed in a careful study of the phototransients in a- As_2Se_3 by Gustave Pfister of Xerox.⁴ Figure 5a is a double logarithmic plot of the normalized current traces in one film of a- As_2Se_3 for a range of transit times encompassing nearly three decades in time. The shape of $I(t)$ is scale invariant (see the discussion in the box on page 30); the curve comes from the theory with $\beta = 0.45$. Pfister observed the dependence of the transit time on the thickness predicted by equation 7 in these measurements. Below, we will see this feature with other transients.

All of the above results depend on the algebraic probability distribution $\psi(t)$ given in equation 3. Is this distribution a reasonable assumption for a disordered material? Under what conditions and material properties does it hold? What is the physical significance of the exponent β ? These queries are best addressed by looking at a simple and commonplace cause of disorder: localized electronic states in the material that act as traps. In the case of extensive multiple trapping, where the total time spent in traps far exceeds the total transit time in the conduction band, one can heuristically write

$$\psi(t) = \sum_i \xi_i W_i e^{-W_i t} \quad (8)$$

Here ξ_i is the probability for capture into the i th trap, and W_i is the release rate from that trap. The distribution in equation 8 is normalized because $\sum_i \xi_i = 1$. If one inserts a relation between the release rate and the energy ϵ of the trap (measured from the band edge)

$$W_i = W_0 \exp(-\epsilon/kT) \quad (9)$$

and assumes a broad (say, exponential) distribution $\rho(\epsilon)$ of these energy levels,

$$\rho(\epsilon) = \rho_0 \exp(-\epsilon/kT_0) \quad (10)$$

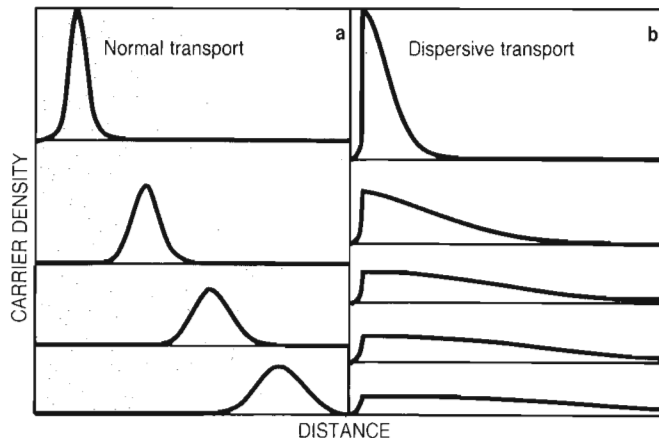
then one can show⁵ that equation 3 holds for $t > \tau$, the mean trap capture time, with

$$\beta = T/T_0 \quad (11)$$

Disorder in the form of a distribution of trap states promotes a spectrum of intrinsic times that limits the transport. In this simple example, the spectrum—that is, the relative release times—is controlled by both the temperature T and the width T_0 of the distribution $\rho(\epsilon)$. The dispersion parameter β is simply the ratio of these controlling factors because the dependence on energy ϵ is the same in equations 9 and 10. When $T > T_0$, the weighting of the release times over the entire distribution is no longer sufficient to allow the rare event (the long release time) to occur often enough to influence the accumulated typical release times. In this regime, $\beta > 1$ and $\langle t \rangle$ is finite, so that the transport becomes quasi-normal, although it is not truly Gaussian until $\beta > 2$.

Intrinsic hydrogenated amorphous silicon provides an excellent example of the multiple trapping mechanism of dispersive transport.⁶ The decay of the current in a-Si:H is purely algebraic for nearly six decades of time (see figure 5b). The two-slope behavior is clearly evident, and the sum of the slopes is -2.01 . The exponent β is found to vary as the ratio T/T_0 , as in equation 11, with T_0 about 30 meV. The energy kT_0 has been interpreted to be the width of the (exponential) conduction-band tail and is in agreement with other determinations of this width.

Hopping involves the tunneling of an electron



Transiting packet of charge. These sequences of “snapshots” represent packets of charge transiting a sample, with time increasing from top to bottom. The normal transport in **a** corresponds to linear evolution in time of the packet’s mean position and gives rise to the current trace shown by curve 1 of figure 3. In **b** the packet’s displacement is controlled by a large dispersion in the arrival time of the carriers at the far electrode. The mean position of the packet is a sublinear function of time and gives rise to the current trace shown by curve 2 in figure 3. **Figure 4**

What Happened to the Infinity

If $\psi(t)$ is a probability density whose first moment $\langle t \rangle$ is infinite, then how can we write temporal relationships and avoid this infinity? The answer is, we calculate moments of $P(l,t)$, the probability of being at site l at time t , and do not calculate the moments of $\psi(t)$ directly. It can be shown that the mean position $l(t)$ may be written as

$$l(t) = \sum l P(l,t) = L^{-1} \left(\frac{l(E) \psi^*(u)}{u[1 - \psi^*(u)]} \right)$$

Here L^{-1} is the inverse Laplace transform, $l(E)$ is the mean step distance, and $\psi^*(u)$ is the Laplace transform of $\psi(t)$. The manner in which

$$\langle t \rangle = \int_0^\infty t \psi(t) dt \Big|_{\lim T \rightarrow \infty}$$

diverges induces a scaling law for $l(t)$. (It diverges as $T^{1-\beta}$ when $\psi(t) \sim t^{-(1+\beta)}$ for large t , or, conversely, $\psi^*(u) \sim 1 - u^\beta$ for small u .) We find asymptotically that the mean position

$$l(t) \sim l(E) L^{-1}(u^{-(1+\beta)}) = l(E) t^\beta$$

The variance from the mean $\sigma(t)$ of $P(l,t)$ is such that $\sigma(t)/l(t)$ is a *constant*, in contrast to $\sigma(t)/l(t)$ for a Gaussian packet, which varies as $t^{-1/2}$. This lies at the heart of the shape invariance of normalized $I(t)$ vs normalized t . Note that $\langle t \rangle = \infty$ does not imply that all the particles wait an infinity of time between hops, so that there is no motion, just as in the St. Petersburg paradox not every gambler wins an infinity of coins.

between localized states. The tunneling rate is a sensitive function of the intersite distance and energy separation of these states. The site-to-site variation in these quantities can result in a wide tunneling-rate spectrum, which can easily generate the algebraic distribution of equation 3 over an appreciable time range. If the disorder in the energy separations is negligible, then the exponent β can be weakly dependent on or even independent of the temperature.

The latter appears to be the case in a recent set of transient current measurements in the well-studied polymeric thin film PVK (polyvinylcarbazole).⁷ Figure 6a again shows the familiar signature of dispersive transport in the double logarithmic plot of the current $I(t)$ in PVK. The data points in figure 6b are the transit times measured for samples of various thicknesses. The black line has a slope of $1/\beta$, where β is determined by the shape of $I(t)$ in figure 6a. The observed scaling behavior of the transit time with thickness is seen to be in agreement with the prediction of equation 7.

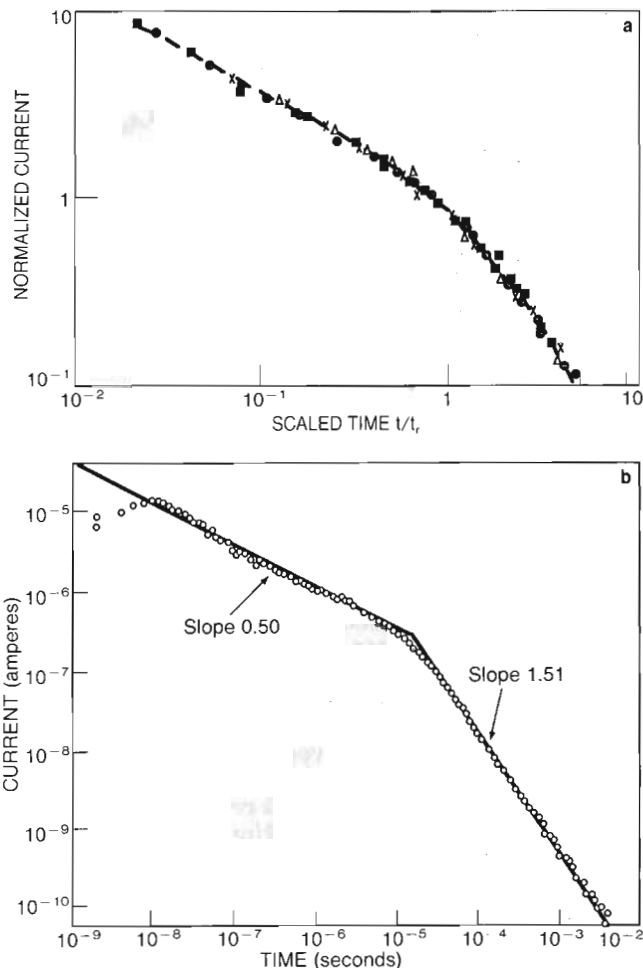
In these measurements the exponent β is observed to be effectively independent of temperature in the experimental range -10°C to $+100^\circ\text{C}$. As the researchers who did this exciting measurement state, “This implies that hole transport in PVK is determined solely by the geometry of the polymer and not by its energetics.” In other words, the effects of the variations in the energy separations on the tunneling rates are negligible.

Silicon dioxide is another important material that exhibits hole transport characterized⁸ by a temperature-independent exponent β . The displacement $l(t)$ of charge is manifested in a measurement of the recovery of the shift in the threshold voltage in the oxide layer of MOS devices (figure 7a). The scaling of the transit time (slope $1/\beta$) with oxide thickness seen in figure 7b is in excellent agreement with the value of $\beta = 0.25$ for the entire three-decade range of transit times.

Most measurements on both hydrogenated amorphous silicon and amorphous chalcogenides are consistent with β proportional to temperature, except at low temperatures. Thus excess carrier transport in amorphous semiconductors is dominated by the omnipresent exponential band tails and is independent of the effects of deep traps.

The great challenge to further theoretical development of the microscopic details of dispersive transport is the problem of hopping in systems with both energy level spread and stochastic geometry. There are no exact solutions to this problem, and numerical simulation results are inconsistent. While hopping is the transport mechanism in a wide variety of polymeric systems, the exact nature of the individual charge-transfer steps has not been resolved.

Transient photocurrents represented in log-log plots. **a:** Plot for amorphous As_2Se_3 . Data points correspond to a superposition of transients covering nearly three decades of transit time. (Adapted from G. Pfister, ref. 4.) **b:** Plot for intrinsic hydrogenated amorphous silicon a-Si:H at 160 K. The current is determined by the sample thickness, applied field and temperature, and decays algebraically over the nearly six decades of observation time of the experiment. (Adapted from ref. 6.) **Figure 5**



The simpler problem of multiple trapping has received considerable attention. Jaan Noolandi and Fred Schmidlin of Xerox showed that the conventional set of coupled kinetic equations describing repeated trapping and release can be cast into the framework of the continuous-time random walk, and they derived the exact form of the probability distribution $\psi(t)$ for multiple trapping.⁹ A. Rudenko and V. Arkhipov of the Moscow Engineering Physics Institute, Thomas Tiedje and Albert Rose of Exxon, and Joseph Orenstein and his coworkers at MIT have presented a useful pictorial representation of the multiple-trapping process based on the idea of a time-dependent demarcation level.⁹ E. Muller-Horsche and his coworkers have developed a reliable procedure for extracting rate distributions from photocurrents that requires measuring the current $I(t)$ over about ten decades of time.¹⁰ Shlesinger has used a particular form of equation 8 to discuss dispersive transport in terms of fractal time,¹¹ a topic to which we will return later.

On the experimental side, while the materials are complex and quite varied, and though details of the transport mechanism remain to be elucidated, the near universality of the main features of their dispersive transport attests to the generality of time-scale invariance.

Very recent transport measurements on a wide class of glassy polymers have revealed¹² a current shape that is "intermediate" between that of curve 1 in figure 3 and those of the curves in figure 5. The current shows a flat initial transient and a long tail for times exceeding the transit time. The normal scaling relation, equation 2, holds for the transit time but not for the variance (see the box on page 30). These features are qualitatively in accord with an exponent β that is less than 2 but not less than 1, a first moment $\langle t \rangle$ that is finite and a second moment $\langle t^2 \rangle$ that is not.³ A suitable distribution $\rho(\epsilon)$ of energy levels can quantitatively account for these new measurements.¹⁰

Relaxation laws

We focused above on the dispersive transport of a single charge and the current it generates. In a natural extension of these ideas, we now consider the dispersive transport of a collection of mobile defects. This type of transport can be the basis for a well-known law for relaxation in a wide variety of random systems.

Peter Debye, with his classic treatment of dielectric relaxation in fluids, set the framework for much of our intuition about relaxation. He derived the law governing how initially aligned small, spherical, dipolar molecules of radius R and dipole moment $\mu(t)$ relax in a fluid of viscosity η and temperature T when the external electric field is removed. The relaxation from an aligned to a random configuration of dipole moments occurs because of random collisions with fluid particles. The relaxation

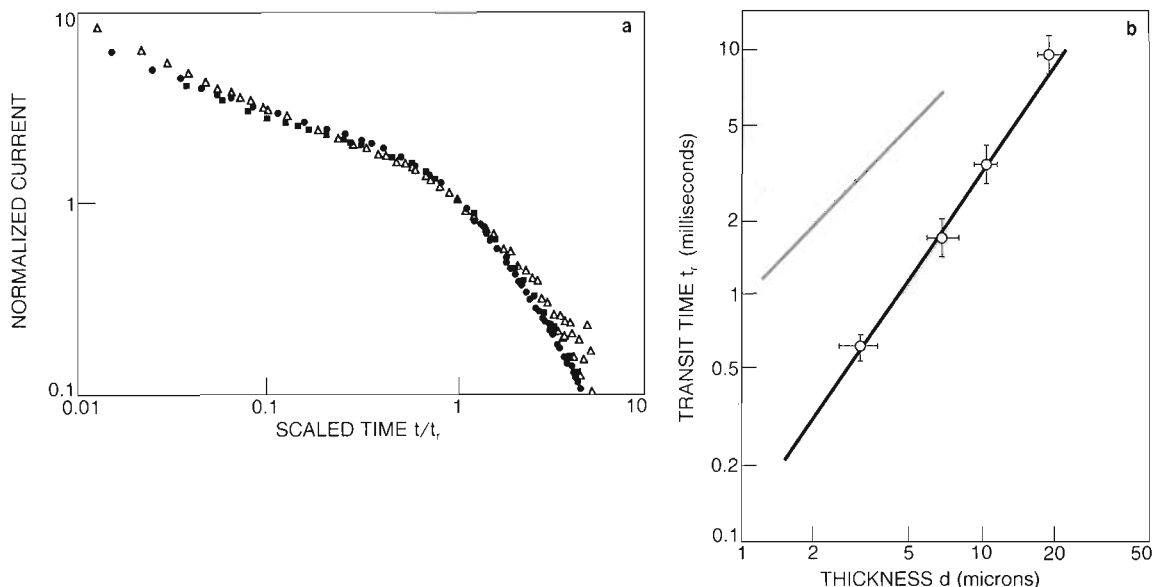
function $\phi(t)$, defined as $\langle \mu(t) \mu(0) \rangle / \langle \mu^2(0) \rangle$, was calculated to be exponential: $\phi(t) = \exp(-t/\tau)$, with $\tau = 4\pi\eta R/kT$. Thus only a single time scale is needed to characterize the relaxation process.

Traditionally, analysis of dielectric relaxation in more complicated systems focused on the complex dielectric constant $\epsilon(\omega)$ and its deviation from the form derived from a single relaxation time.¹³ A change of focus from frequency to time—from $\epsilon(\omega)$ to $\phi(t)$ —occurred in 1970 when Graham Williams and David Watts¹³ found empirically that the following form fit data for glassy and polymeric materials, including polyethylacrylate and propylene oxide, with β between 0 and 1:

$$\phi(t) = \exp[-(t/\tau)^\beta] \quad (12)$$

(Andrez Plonka has made an extensive survey of the role of this relaxation function $\phi(t)$ in investigating the time-dependent reactivity of trapped species in condensed matter.¹⁴) In the past few years this form for $\phi(t)$ has been used to fit an ever widening variety of experimental data, including data from mechanical, nmr, dielectric, enthalpic, volumetric, dynamic light scattering, magnetic relaxation and reaction kinetics measurements. It was recently shown to account for the relaxation of the localized electronic structure of a-Si:H, which we will describe below.¹⁵

It was in a study of remnant magnetization that the expression "stretched exponential" was born to describe equation 12, and the nomenclature has stuck. The modern flurry of activity actually obscures the fact that



Signature of dispersive transport in polyvinylcarbazole and resulting scaling behavior of the transit time. **a:** Superposition master plot of $I(t)$ obtained at a number of electric field strengths and temperatures. The value of the exponent β is 0.6. **b:** Dependence of transit time on sample thickness. The black line is drawn with slope $1/\beta$, where β is 0.6. The colored line has the slope of 1 that is expected for normal transport. (Adapted from ref. 7.) **Figure 6**

the stretched exponential was introduced in 1863 to describe mechanical creep in glassy fibers.¹⁶ (See the box on page 34.)

The stretched exponential was a subject of interest in the "Brinkman report," which stated¹⁷:

There seems to be a universal function that slow relaxations obey. If the system is driven (or normally fluctuates) out of equilibrium, it returns according to the formula $\exp[-(t/\tau)^\beta]$ Unfortunately, this is not a mathematical expression that is frequently encountered in physics, so little idea exists of what the underlying mechanisms are.

There are now several derivations of the stretched exponential for systems in three dimensions, involving diverse concepts such as percolation, hierarchical relaxation of constraints, and multipolar interaction transitions.¹⁸ We will consider a mechanism based on a reaction picture involving the *dispersive transport of defects*. Although this concept and the others just mentioned are dissimilar, a common mathematical structure connects them.¹⁹

In the Debye model, the underlying mechanism of relaxation was fluid particles randomly hitting polar molecules. Consider now a model for a glass in which mobile defects hit a frozen-in dipole and instantaneously cause its relaxation. Sivert Glarum of Bell Laboratories used a model of this type in which a defect undergoes Brownian motion in one dimension.²⁰ We generalize Glarum's work by allowing for a finite concentration c of defects in three dimensions and, most importantly, by treating their motion as dispersive.¹¹ What is the probability that the "dipole" will first be reached at time t by one of the N diffusing defects in a volume N/c ? Because each defect moves independently, the probability is a product of N factors that for large N becomes an exponential:

$$\phi(t) = \exp[-cS(t)]$$

Here $S(t)$ is the number of distinct sites a defect visits in a time t .

In three dimensions,

$$S(t) \sim \begin{cases} t, & \text{for } \langle t \rangle \text{ finite} \\ t^\beta, & \beta < 1, \text{ for } \langle t \rangle \text{ infinite} \end{cases}$$

In one dimension $S(t)$ goes as $t^{1/2}$ for $\langle t \rangle$ finite and $t^{\beta/2}$ for $\langle t \rangle$ infinite.

The first case occurs when the mean time $\langle t \rangle$ between

defect hops is finite, and the latter case for dispersive transport where $\psi(t) \sim t^{-(1+\beta)}$, $\beta < 1$. Within the defect diffusion model, we obtain either Debye relaxation (for finite $\langle t \rangle$) or stretched-exponential relaxation (for infinite $\langle t \rangle$). In the latter case, any details that do not change the condition $\langle t \rangle = \infty$ are irrelevant. Thus one answer to the question of why the stretched exponential is so widespread is that it can be a probability limit distribution.

The defect diffusion derivation of the stretched exponential calls for the movement of defects. But what is a defect? In general, this is a difficult question to answer, although many possibilities have been suggested for specific materials. Let us look at two distinct cases. The first is the practical engineering polymer polycarbonate, a high-impact thermoplastic resin. It displays ductility in the glass state, unlike most polymers, which are brittle. Much speculation has centered on the origin of this plastic flow, and a variety of solid-state nmr line-shape and relaxation experiments have provided, for the first time, structural details of molecular motion in the glass.²¹ In particular, carbon-13 and deuterium line-shape measurements reveal that aromatic ring motions occur readily in the solid, with little or no disturbance of the backbone direction or orientation. A mobile carbonate (CO_3) bond is considered here to be the "defect" whose movement is responsible for inducing the mechanical, nmr and dielectric relaxation in this glassy polymer.²² Indeed, all three types of measurements find stretched-exponential behavior (equation 12), with an exponent β of 0.15. (See the figure in the box on page 34.) The low value of β may be connected to the quasi-one-dimensional motion of the mobile bond.

The second example comes from a recent study¹⁵ of the relaxation of the nonequilibrium electronic and

atomic structures of doped a-Si:H. In this study, which has provided considerable evidence for the physical mechanism we have been discussing, James Kakalios and his coworkers at Xerox examined the relaxation of the temperature-dependent densities of dangling bond defects and donor states in rapidly cooled samples of n-type a-Si:H (and acceptor states in p-type material), as probed by monitoring the time dependence of the band-tail states. They found the relaxation to be well described by a stretched exponential with exponent β varying linearly with temperature. (The room temperature value of β for n-type a-Si:H is 0.45.) A good candidate for the diffusing "defects" that account for the kinetics of the structural relaxation is the bonded hydrogen. In other studies, Kakalios and his coworkers have established that the hydrogen exhibits dispersive diffusion. Moreover, they have made the important observation that the $\beta(T)$ parameter determined from the measurement of hydrogen diffusion is entirely consistent with the $\beta(T)$ obtained by fitting the relaxation data to a stretched exponential.

A concluding illustration

The subtlety of dispersive transport involves not only a broad range of times but the relative probabilities of events with these times occurring. To illustrate this point, let us return to our canonical experiment, transport of a pulse of excess charge across a film of a disordered solid. Suppose that the spread in arrival times to the back electrode is due to the stochastic delays introduced by carrier trapping. If a finite fraction of the pulse can arrive without being trapped, then one can define a time scale t_r for the transit by equation 2, where μ_d is in this case the band mobility. The trapped fraction of the pulse typically has a mean release time t_R that is greater than t_r , and is therefore "lost" to the transiting pulse on the time scale of t_r . However, by increasing the probability of an encounter with the traps (by increasing the trap density, for example), one can have $t_R \ll t_r$, where t_r , the time scale of the measurement, is now the average accumulation of

release times before arrival at the back electrode, and μ_d in equation 2 is now the conventional "drift" mobility. The "intermediate" situation, where a well-defined time t_r becomes blurred, can arise when t_r is in the midst of a range of release times. This simple example shows that besides the range, we must be careful to consider also the encounter probability.

A special case of equation 8 will clarify the remaining discussion. Consider a discrete set of trapping levels indexed by an integer n , such that¹¹

$$\psi(t) = \frac{1-a}{a} \sum_{n=1}^{\infty} a^n b^n \exp(-b^n t) \quad (13)$$

Here each level n has a power-law weighting (a^n , $a < 1$) and a release time (b^{-n} , $b < 1$). The nondimensional mean time $b\langle t \rangle$ of the distribution given in equation 13 is

$$b\langle t \rangle = \frac{1-a}{a} \sum_{n=1}^{\infty} a^n b^{-n+1} \quad (14)$$

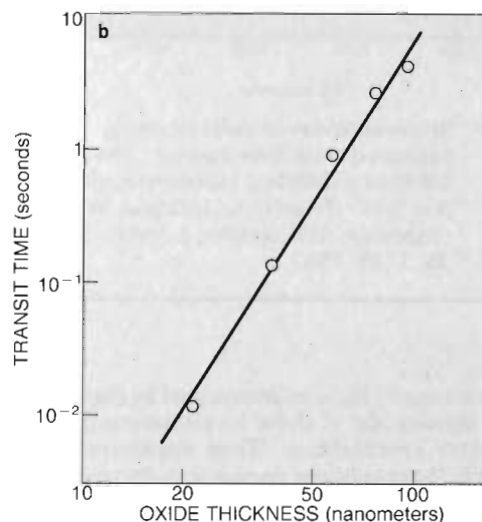
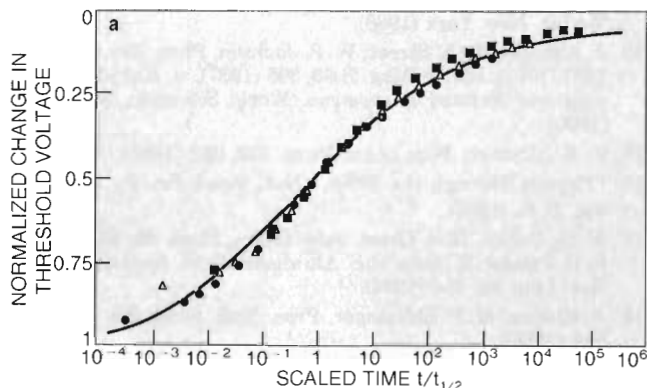
For $a > b$, $b\langle t \rangle = \infty$ and the asymptotic decay is $\psi(t) \sim t^{-(1+\beta)}$, with

$$\beta = \frac{\ln a}{\ln b} \quad (15)$$

which is in the form of a fractal dimension.¹¹ For $b > a$, the mean time $b\langle t \rangle$ is finite. This example clearly shows the interplay between a wide range of times $\{b^{-n}\}$ and the probability a^n of encountering each of these times. One can rewrite equation 11 as¹⁰

$$\beta = \frac{T}{T_0} = \frac{-\varepsilon/kT_0}{-\varepsilon/kT} = \frac{\ln[\rho(\varepsilon)/\rho_0]}{\ln[W(\varepsilon)/W_0]} \quad (16)$$

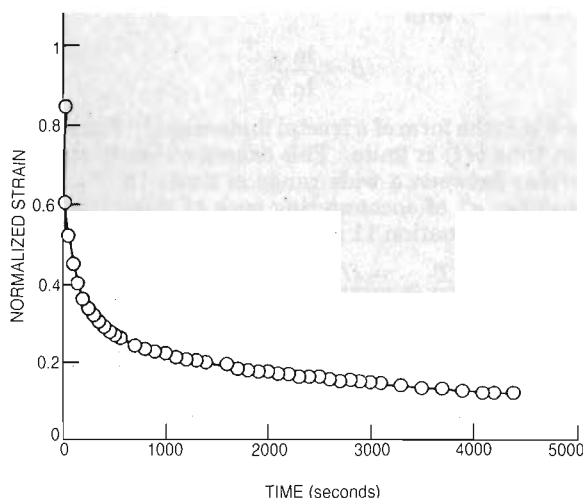
The form for β is the same as for the discrete case in equa-



MOS device behavior. **a:** Recovery of the threshold voltage of a silicon MOS device for a range of thicknesses. The curve is obtained from theory. The recovery is due to the dispersive transport of holes across the oxide layer. **b:** Dependence of transit time on thickness of the oxide layer in a silicon MOS device. The solid line has a slope of $1/\beta$, where β is determined from the recovery of the threshold voltage of the device. Here β is 0.25. (Adapted from ref. 8.) **Figure 7**

Mechanical Relaxation

When Robert Hooke in 1678 presented his law according to which a restoring force is linearly proportional to elongation, it was appreciated that exceptions existed. One area where Hooke's law did not apply was creep and stress relaxation in solids. In 1829 Vicat, who surveyed the sagging of wires and the general stability of suspension bridges across the Rhone, initiated a scientific study of creep. The problem of the viscoelastic response of solids has since challenged a number of distinguished physicists, including Gaspard Gustave de Coriolis, Claude-Louis-Marie Navier, Karl Friedrich Gauss, Wilhelm Weber, James Clerk Maxwell and Ludwig Boltzmann. In 1854 Rudolf Kohlrausch introduced the stretched exponential in his study of the loss of charge in Leyden jars. In his experiments on magnetic forces around the same time, Weber studied creep in the silk threads he used to suspend magnetic bars. In 1863 Frederick Kohlrausch (following the experiments of his father Rudolf and the work of Weber) used the stretched exponential as an empirical fit for creep and relaxation data in silk and glass fibers and in rubber.¹⁶ As the figure below indicates, modern experiments on mechanical behavior, which employ optical birefringence measurements along with the traditional stress-strain measurements, agree well with Frederick Kohlrausch's findings.



Strain recovery in polycarbonate, measured using birefringence. The data are fit to a stretched exponential with $\beta = 0.15$. (From D. G. LeGrand, W. V. Olszewski, J. T. Bendler, *J. Polym. Sci.* **25**, 1149, 1987.)

tion 15. The rate range $\{W(\epsilon)\}$ is determined by the energy levels, but the density $\rho(\epsilon)$ of these levels determines the relative encounter probabilities. Thus dispersive transport arises when these relative encounters decrease at a rate that is carefully balanced by the increase in the delay times—that is, when $a > b$. This subtlety lies at the heart of the algebraic behavior of $\psi(t)$. It is also this same interplay—between the frequency of occurrence of the various sizes of correlated regions and the sizes of these regions—that accounts²³ for critical phenomena near T_c .

Finally, if we take the limits $a \rightarrow 1/2$ and $b \rightarrow 1/2$ in equation 14, then the mean time $b\langle t \rangle$ is simply the

(diverging) mean winnings of the coin-toss game that gave rise to the original St. Petersburg paradox.

* * *

We gratefully acknowledge the suggestions and critical reading of the manuscript by Martin A. Abkowitz, Alton H. Clark, William A. Curtin, Jon H. Harris, Leonid A. Turkevich, Joseph Klafter and Richard Zallen.

References

1. I. Todhunter, *A History of the Mathematical Theory of Probability*, Cambridge U. P., Cambridge, England (1865).
2. E. W. Montroll, G. H. Weiss, *J. Math. Phys.* **6**, 167 (1965).
3. E. W. Montroll, H. Scher, *J. Stat. Phys.* **9**, 101 (1973). M. F. Shlesinger, *J. Stat. Phys.* **10**, 421 (1974). H. Scher, E. W. Montroll, *Phys. Rev. B* **12**, 2455 (1975).
4. M. E. Scharfe, *Phys. Rev. B* **2**, 5025 (1970). G. Pfister, *Phys. Rev. Lett.* **33**, 1474 (1974).
5. H. Scher, in Proc. Seventh Int. Conf. on Amorphous and Liquid Semiconductors, Edinburgh, unpublished (1977), p. 209. G. Pfister, H. Scher, *Adv. Phys.* **27**, 747 (1978).
6. T. Tiedje, in *Semiconductors and Semimetals*, vol. 21C, J. Pankove, ed., Academic, New York (1984), p. 207.
7. F. C. Bos, D. M. Burland, *Phys. Rev. Lett.* **58**, 152 (1987).
8. H. E. Boesch Jr, F. B. McLean, J. M. McGarrity, P. S. Winokur, *IEEE Trans. Nucl. Sci.* **25**, 1239 (1978). F. B. McLean, H. E. Boesch Jr, T. R. Oldham, in *Ionizing Radiation Effects in MOS Devices and Circuits*, T. P. Ma, P. V. Dressendorfer, eds., Wiley, New York (1989), p. 87.
9. F. W. Schmidlin, *Phys. Rev. B* **16**, 2362 (1977). J. Noolandi, *Phys. Rev. B* **16**, 4466 (1977). A. I. Rudenko, V. I. Arkhipov, *Philos. Mag.* **39**, 465 (1979). T. Tiedje, A. Rose, *Solid State Commun.* **37**, 49 (1981). J. Orenstein, M. Kastner, V. Vaninov, *Philos. Mag. B* **46**, 23 (1982).
10. E. Muller-Horsche, D. Haarer, H. Scher, *Phys. Rev.* **35**, 1273 (1987).
11. M. F. Shlesinger, *Annu. Rev. Phys. Chem.* **39**, 269 (1988).
12. M. Abkowitz, M. J. Rice, M. Stolka, *Philos. Mag. B* **61**, 25 (1990).
13. R. Cole, *Annu. Rev. Phys. Chem.* **40**, 1 (1989). G. Williams, D. C. Watts, *Trans. Faraday Soc.* **66**, 80 (1970).
14. A. Plonka, *Time-Dependent Reactivity of Species in Condensed Matter*, Lecture Notes in Chemistry 40, Springer-Verlag, New York (1986).
15. J. Kakalios, R. A. Street, W. B. Jackson, *Phys. Rev. Lett.* **59**, 1037 (1987); *Philos. Mag. B* **56**, 305 (1987). J. Kakalios, *Hopping and Related Phenomena*, World Scientific, Singapore (1990).
16. F. Kohlrausch, *Pogg. Ann. Phys.* **119**, 352 (1863).
17. "Physics Through the 1990s," *Natl. Acad. Sci. P.*, Washington, D. C. (1986).
18. M. H. Cohen, G. S. Grest, *Adv. Chem. Phys.* **48**, 455 (1981). R. G. Palmer, D. Stein, E. S. Abrahams, P. W. Anderson, *Phys. Rev. Lett.* **53**, 958 (1984).
19. J. Klafter, M. F. Shlesinger, *Proc. Natl. Acad. Sci. USA* **83**, 848 (1986).
20. S. Glarum, *J. Chem. Phys.* **33**, 1371 (1960).
21. K. L. Li, P. T. Inglefield, A. A. Jones, J. T. Bendler, A. D. English, *Macromolecules* **21**, 2940 (1988).
22. J. T. Bendler, *Ann. N. Y. Acad. Sci.* **371**, 299 (1981). A. A. Jones, J. F. O'Gara, P. T. Inglefield, J. T. Bendler, A. F. Yee, K. L. Ngai, *Macromolecules* **16**, 658 (1983).
23. R. Zallen, *The Physics of Amorphous Solids*, Wiley, New York (1983), chaps. 4–6. ■